Vilniaus universiteto

Fizikos fakulteto

Lazerinių tyrimų centras

Maksim Sidorenko

Transverse modes of spectrally broadened femtosecond radiation in gas-filled hollow-core fiber

Bakalauro studijų baigiamasis darbas

Šviesos technologijos

Studentas Maksim Sidorenko

Darbo vadovas Doc. Rytis Butkus

Instituto/Centro direktorius/atstovas Prof. Aidas Matijošius

Vilnius 2023

Table of contents

Abstract

Noble gas filled hollow-core fibers are often used for spectral broadening of femtosecond laser radiation. This work presents the investigation of transverse modes, obtained by broadening the spectrum of Ti-Sapphire 800 nm 50 fs laser radiation. The laser beam was focused into the fiber by 3 different lenses: of 2, 2,5 and 3 m focal distance. With each lens, the dependence of spectral broadening on Ar pressure inside the fiber was investigated. Higher pressures resulted in wider spectra, as well as having a lens with shorter focal distance equipped. Transverse modes were more symmetric when laser beam was focused with a lens of a longer focal distance, however the losses were higher.

Abstract (LT)

Inercinių dujų užpildyti tuščiaviduriai šviesolaidžiai dažnai naudojami femtosekundinės lazerio spinduliuotės spektro išplėtimui. Šiame darbe pristatomas skersinių modų, gautų išplėtus Ti-Safyro 800 nm 50 fs lazerio spinduliuotės spektrą, tyrimas. Lazerio spinduliuotė buvo sufokusuotas į pluoštą 3 skirtingais lęšiais: 2, 2,5 ir 3 m židinio nuotolio. Su kiekvienu lęšiu buvo ištirta spektro išsiplėtimo priklausomybė nuo Ar slėgio šviesuolaidyje. Didesnis slėgis lėmė platesnius spektrus, taip pat kaip ir nauduojant trumpesnio židinio nuotolio lęšį. Skersinės modos buvo simetriškesnės, kai lazerio spinduliuotė buvo sufokusuota su didesnio židinio nuotolio lęšiu, tačiau nuostoliai buvo didesni.

Introduction

Many studies were done in femtosecond laser radiation spectrum broadening. The need for these studies is to find methods of achieving ultrashort pulses down to 10 fs. Different scientific resources promote the use of noble gas filled hollow-core optical fibers for pulse spectral broadening, presenting the more advantageous technique, compared to the use of single-mode fibers, which are limited to lower energy (nJ) [1].

The aim of the work is to investigate the transverse modes of spectrally broadened femtosecond radiation in gas-filled hollow core fiber, explain the differences in resulting modes and spectra, and find the best experimental setup configuration for the further uses of spectrally broadened radiation.

Tasks: 1) Using several lenses with different focal distances, investigate the transverse modes and spectra at different pressures inside the hollow-core fiber;

2) Using the interference filters, investigate the transverse modes at different wavelengths;

3) Compare the results and explain the reasons behind mode shape differences.

Theoretical introduction

The relation between laser pulse compression and spectral broadening can be explained with the following equations [2,3]: First, we describe the Gaussian pulse envelope as a function of electric field:

$$E(t) = E_0 \cdot e^{i\omega_0 t} \cdot e^{-\frac{t^2}{\sigma_t^2}}, \tag{1}$$

where E_0 – electric field constant, w_0 – central frequency and $e^{-\frac{t^2}{\sigma_t^2}}$ defines the Gaussian envelope. After changing to frequency domain by applying the Fourier transformation, the equation (1) appears as:

$$E(\omega) = \sqrt{\frac{\sigma_t^2}{2}} \cdot E_0 \cdot e^{-\frac{\sigma_t^2}{4}(\omega-\omega_0)^2}, \tag{2}$$

the spectral intensity is given by:

$$S(\omega) = |E(\omega)|^2 = \frac{4\ln 2}{\Delta\omega^2} \cdot {E_0}^2 \cdot e^{-4\ln(2)\frac{(\omega-\omega_0)^2}{\Delta\omega^2}}, \tag{3}$$

where $\Delta\omega = \frac{2\sqrt{2\ln 2}}{\sigma_t} = \frac{4\ln 2}{\tau}$, and τ is a pulse duration at FWHM. Equation (2) can include a phase function $e^{i\phi(\omega)}$ where $\phi(\omega)$ is a spectral phase, which can be expander in Taylor series:

$$\phi(\omega) = \phi_0 + \phi_1 \cdot (\omega - \omega_0) + \frac{\phi_2}{2}(\omega - \omega_0)^2 + \cdots . \tag{4}$$

The 2-nd order part of this Taylor series creates a linear chirp to the pulse, the varying instantaneous frequency is described by Equation (5).

$$\omega(t) = \omega_0 + \frac{4\phi_2}{\sigma_t^4 + 4\phi_2^2} \cdot (t - t_0), \tag{5}$$

which means that the pulse envelope will contain more frequencies, thus, results in wider spectra.

The principle behind the spectral broadening inside a noble gas filled hollow-core optical fiber is self-phase modulation [1,4,5,6]. This effect occurs due to a nonlinear response of refractive index to electric field, which is known as Kerr effect. Equation 6 reveals refractive index dependence on intensity [2]:

$$n(t) = n_0 + n_2 \cdot I(t) , \tag{6}$$

where $I(t) = |E(t)|^2$, n_2 - nonlinear refractive index. The instantaneous frequency is now described as:

$$\omega(t) = \omega_0 - \frac{\omega}{c} n_2 \frac{\delta I(t - \frac{z}{v_g}))}{\delta t} L , \tag{7}$$

where *z* – distance from beam waist, $v_g = \frac{c}{n(\omega) + \omega\frac{\delta n}{\delta\omega}}$ – group velocity and L – pulse propagation distance in a nonlinear medium. For a hollow-core fiber, noble gases serve as a nonlinear medium, and in the case of this experiment – argon [7].

Experimental setup

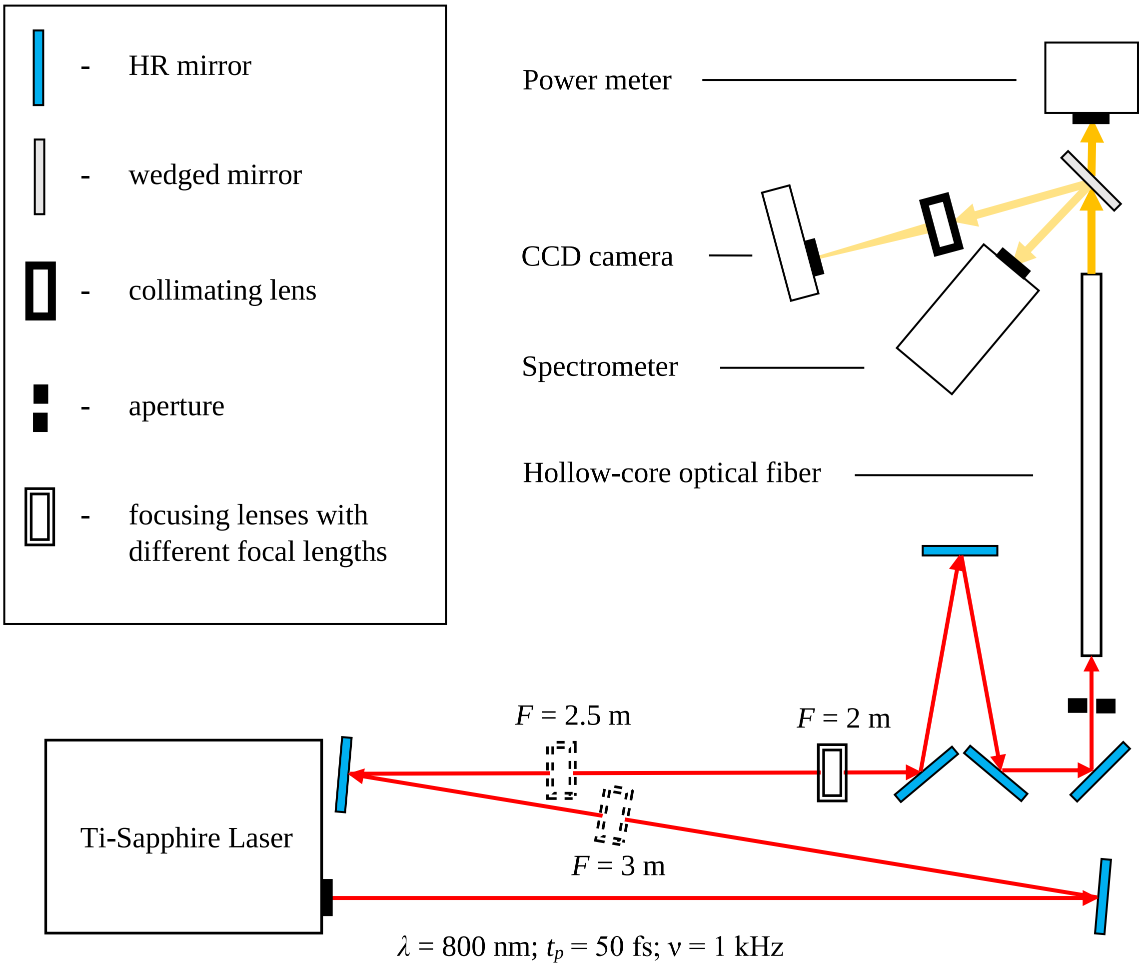

Fig. 1: Experimental setup diagram. λ – laser wavelength; t_p – pulse temporal width, ν – pulse repetition rate.

The experimental setup is equipped with Ti-Sapphire femtosecond laser. The average output power used in the experiment is 430 mW. The measured beam waist diameter is 10.7 mm at $1/e^2$. The 2 m long hollow-core optical fiber has an inner diameter of 500 micrometers, therefore, there is a limitation for using longer focal distance lenses, which focus the laser beam to a larger spot. The beam waist diameter at the focal point of the lens shold not exceed the diameter of the fiber, since each lens was placed to match the beam waist position and the fiber input-face. Thus, lenses with 2, 2.5, 3 and 4 meter focal lengths were tested to find out if the condition above is satisfied. The measurement was performed without the laser beam going through the optical fiber, the setup configuration was different than the one shown in Fig. 1.

(a) Transverse mode size dependence on the distance from a focal point

(b) Transverse mode size dependence on the distance from a focal point (scaled)

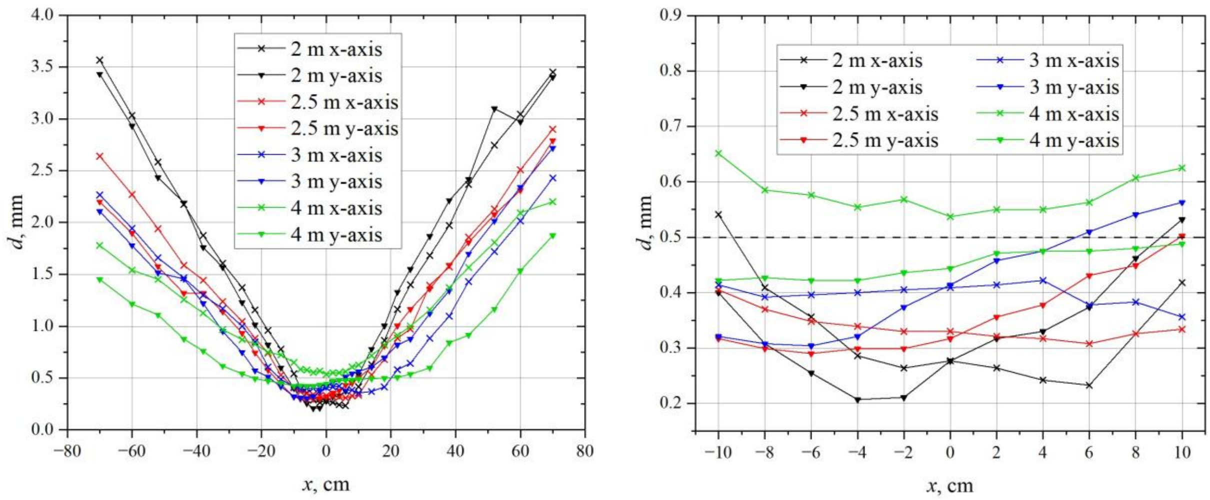

Fig. 2: Transverse mode size (measured at $1/e^2$) variation around the focal point. The focal point (0 on the x-axis) represents the point where the smallest and most symmetric transverse mode image was observed with a CCD camera. Graph **(a)** depicts all the distances at which the mode size was measured to represent the overall dependence, **(b)** is downscaled to ± 10 cm to clearly depict the sizes of beam waists, a dashed horizontal line represents the limiting diameter of interest (fiber core diameter).

From figure 2, it is noticible that the laser beam is astigmatic, the focal lengths for x and y axes differ by 10-12 cm. The smallest width of a transverse mode achieved with a $F = 4$ m lens clearly exceeds 0.5 mm, hence, this lens will not be used in the experiment, since it would result in major power losses as the laser beam would not fully enter the optical fiber, and also could result in damaging the fiber cladding. For the same reason, it was very important to precisely adjust the mirrors angles to perfectly align the laser beam and the fiber core.

Before entering the fiber, the laser beam experiences energy losses due to the optical elements – 6 mirrors and a lens (the diameter of an opened aperture exceeds the beam waist diameter, hence there are no losses from the aperture). Laser beam energy was measured at the laser output and at the fiber entrance, as a result, the losses made up ≈ 5% with $F = 2$ m lens installed and ≈ 10 % with $F = 2.5$ m or $F = 3$ m lenses. The reason behind such difference is that the 2 m focal length lens has an anti reflecting surface, which helps to reduce losses. The transmission coefficient of the wedged mirror made up 90%, this will be important while calculating the losses in optical fiber.

Experiment and results

The experiment was conducted in the following way: First, the lens with a 2-meter focal distance was installed into the laser optical path, the mirror angles were adjusted, so the laser beam would precisely enter the fiber core while going through the aperture. Second, the hollow-core fiber was evacuated, the tilts of the ends were adjusted to prevent any slightest bends, ensuring the propagation with the least losses. With a CCD camera, the image of a transverse mode is observed (Figure 3).

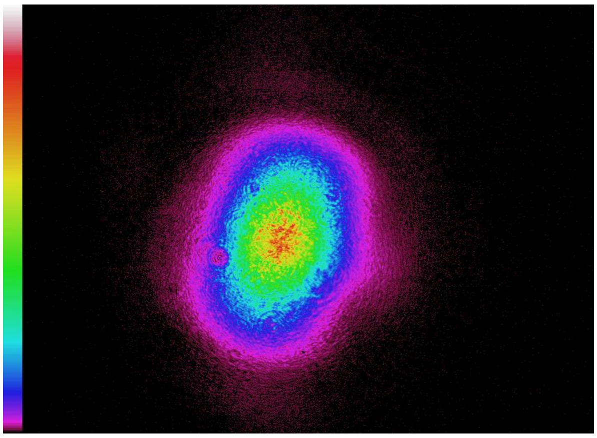

Fig. 3: Transverse mode image.

F = 2 m lens;

P_{Ar} = 0 bar;

x = 1.434 mm, y = 1.993 mm

x – height at peak intensity/e^2, y – width at peak intensity/e^2. The above parameters will be denoted identically in the following figures.

The next step was to fill the optical fiber with Ar gas. Before measuring the spectra and observing the transverse mode at a specific Ar pressure, the dependence of the mode shape on pressure was measured (Figure 4).

(a) P_{Ar} = 0 bar

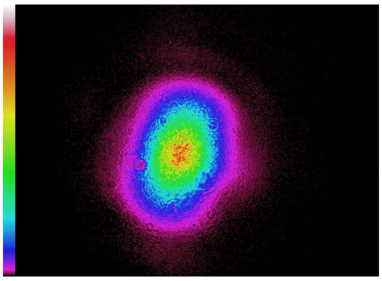

(b) P_{Ar} = 0.35 bar

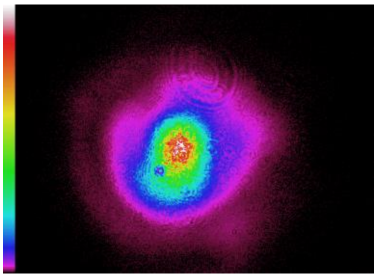

(c) P_{Ar} = 0.6 bar

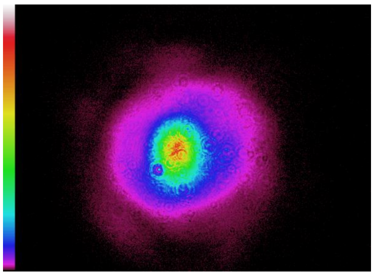

(d) P_{Ar} = 0.75 bar

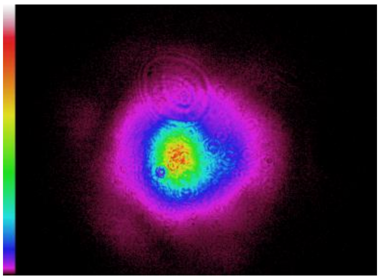

(e) P_{Ar} = 0.95 bar

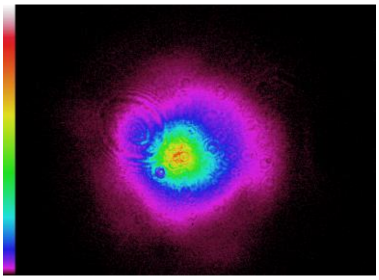

(f) P_{Ar} = 1.2 bar

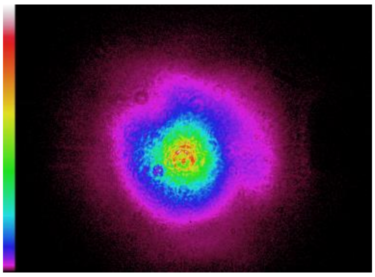

Fig. 4: Transverse modes observed at different Ar pressures: **(a)** – vacuum, **(b)** – 0.35 bar, **(c)** – 0.6 bar, **(d)** – 0.75 bar, **(e)** – 0.95 bar, **(f)** – 1.2 bar. The ends of a fiber were not adjusted after increasing the pressure.

As the Ar gas pressure in the hollow-core optical fiber increases, the spectrum gets wider, to depict this dependence, the spectrum was also measured at each pressure (Figure 5). When observing the laser beam, as the pressure increases, it becomes brighter and acquires red and yellow colors, since the part of the spectrum widens towards the visible light.

(a) Spectrum dependence on Ar pressure **(b)** Spectrum width dependence on Ar pressure

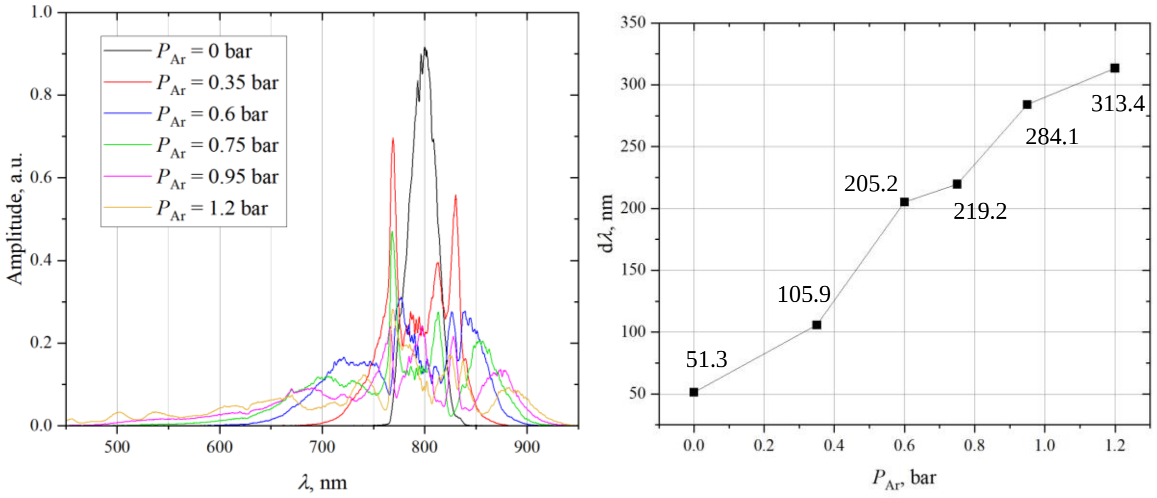

Fig. 5: Spectrum dependence on the Ar pressure inside the hollow-core fiber. Graph **(a)** depicts the spectra at each pressure value, showing the change in width and different peak values. **(b)** demonstrates the linear dependence of spectrum width on the pressure, the width is measured at the peak/e^2, since there is no central wavelength at higher pressures, instead, different peaks separated by 50 nm and more, so the FWHM would not determine the full width of the spectrum.

(a) Adjusted fiber **(b)** Unadjusted fiber

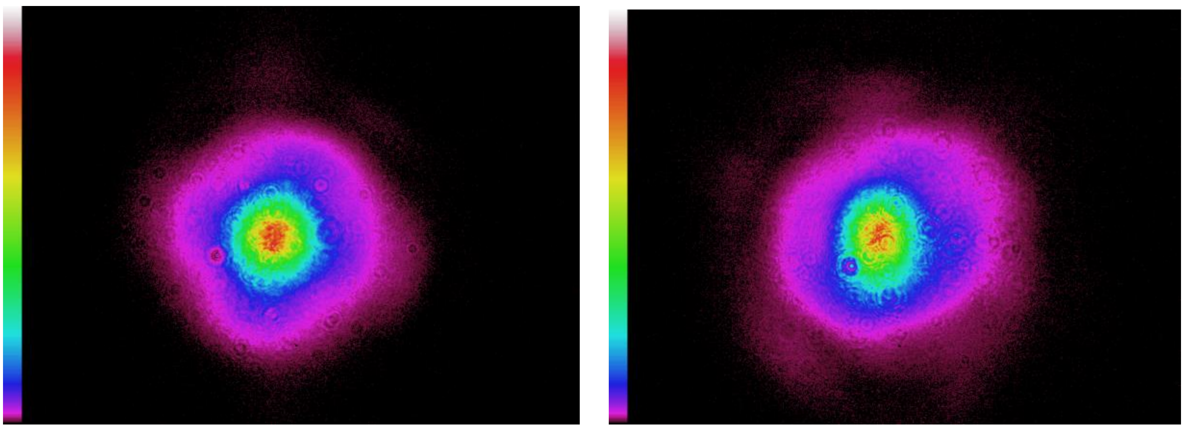

Fig. 6: (a) Transverse mode after adjusting the fiber ends at P_{Ar} = 0.65 bar; x = 1.311 mm, y = 1.316 mm; 2-meter focal distance lens equipped. **(b)** Image taken from Figure 4; x = 1.223 mm, y = 1.496 mm. **(c)**. The pressure difference of 0.05 bar is too negligible to deform the mode, so **(a)** and **(b)** are comparable.

Since the fiber gets slightly deformed as the pressure increases, changing the transverse mode, it is required to adjust the fibers ends at each working pressure. Figure 6 shows the difference in mode shape when the fiber is unadjusted or adjusted at the same pressure. Comparing Figure 6 (a) and (b), it is obvious that figure (a) demonstrates better symmetry, proofing the necessity of adjusting the fiber at each pressure. As it is done, there are also slight changes to the spectrum shape (Figure 7).

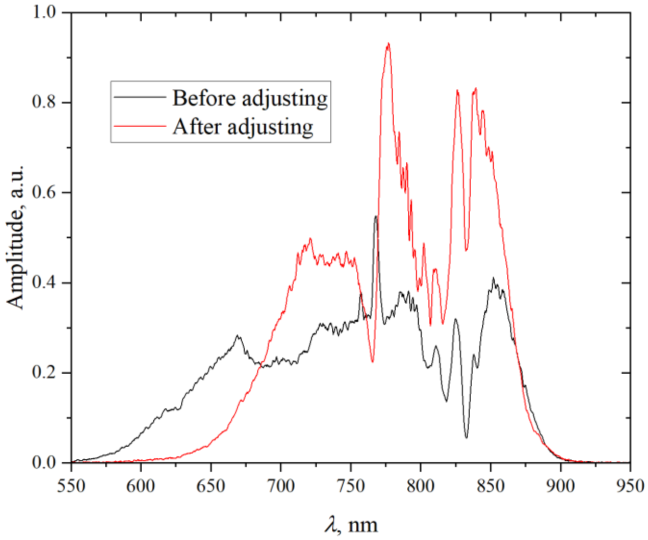

Fig. 7: Difference in spectrum shape before and after adjusting the fiber. The spectra are related to transverse modes shown in Figure 6.

The next step of the experiment was to maintain a certain Ar pressure, when the visible light is generated, adjust the optical fiber to obtain the most symmetrical transverse mode, and observe the modes using interference filters for different wavelengths (placed in front of CCD camera). The filter transmits 10 nm (FWHM) width part of the spectrum with a specific central wavelength. Figure 9 demonstrates the modes of different parts of the spectrum. The fundamental mode, obtained without the interference filters is presented in Figure 6 (a). Without changing the lens, the measurement is repeated with a higher pressure of Ar gas, the results are presented in Figure 10, and the funtamental mode at 1 bar in Figure 8. Same experiment procedure (except for measuring the transverse mode dependence on Ar pressure) was repeated for F = 2.5 m and F = 3 m lenses, the following results are presented in Figure 14 and Figure 15 (fundamental modes obtained without using interference filters), as well as in Figure 11, Figure 12 and Figure 13 (spectra and modes of filtered radiation).

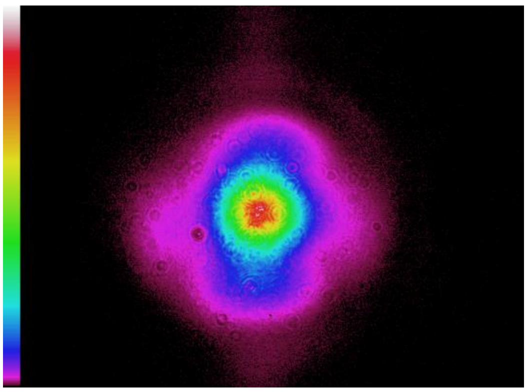

Fig. 8: Transverse mode image.

F = 2 m lens;

P_{Ar} = 1 bar;

x = 1.276 mm, y = 1.558 mm

(a) 700 nm filter

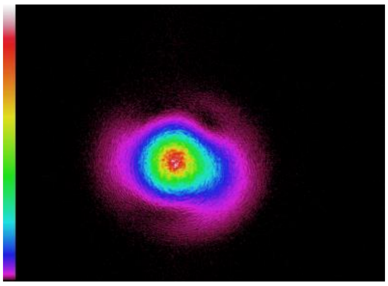

(b) 750 nm filter

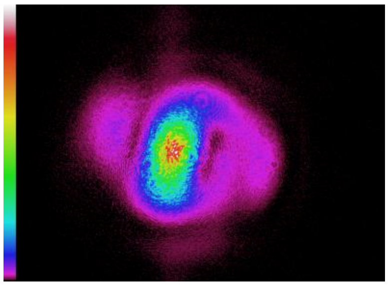

(c) 800 nm filter

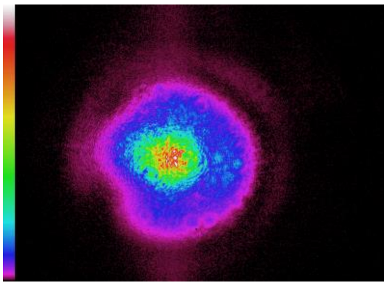

(d) 850 nm filter

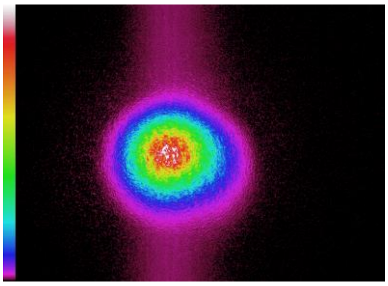

(e) 900 nm filter

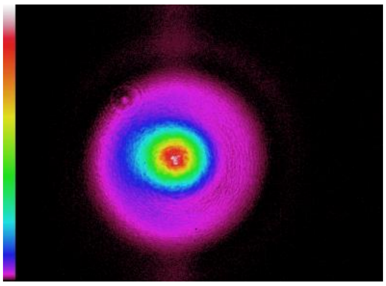

(f)

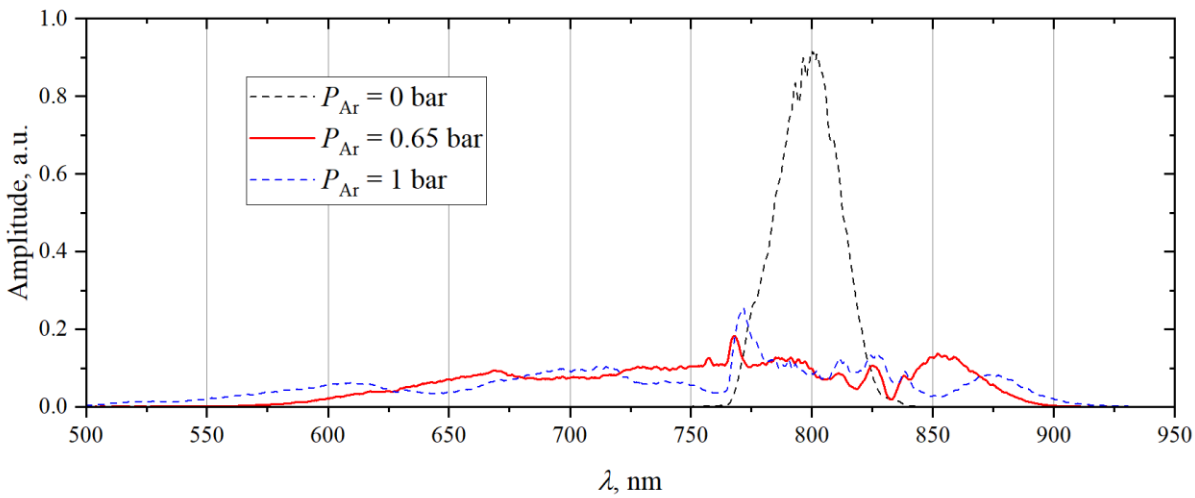

Fig. 9: Images **(a)** – **(e)** depict transverse modes with all the light filtered except for a denoted wavelength. The graph **(f)** visualizes spectra at vacuum and two different pressures. The images of the modes are related to spectrum which is visualized as a solid curve (P_{Ar} = 0.65 bar). The focal distance of the lens is 2 m.

Sizes of transverse modes: **(a)** x = 1.571 mm, y = 1.179 mm; **(b)** x = 0.92 mm, y = 1.804 mm; **(c)** x = 1.487 mm, y = 1.333 mm; **(d)** x = 2.275 mm, y = 1.925 mm; **(e)** x = 1.553 mm, y = 1.320 mm.

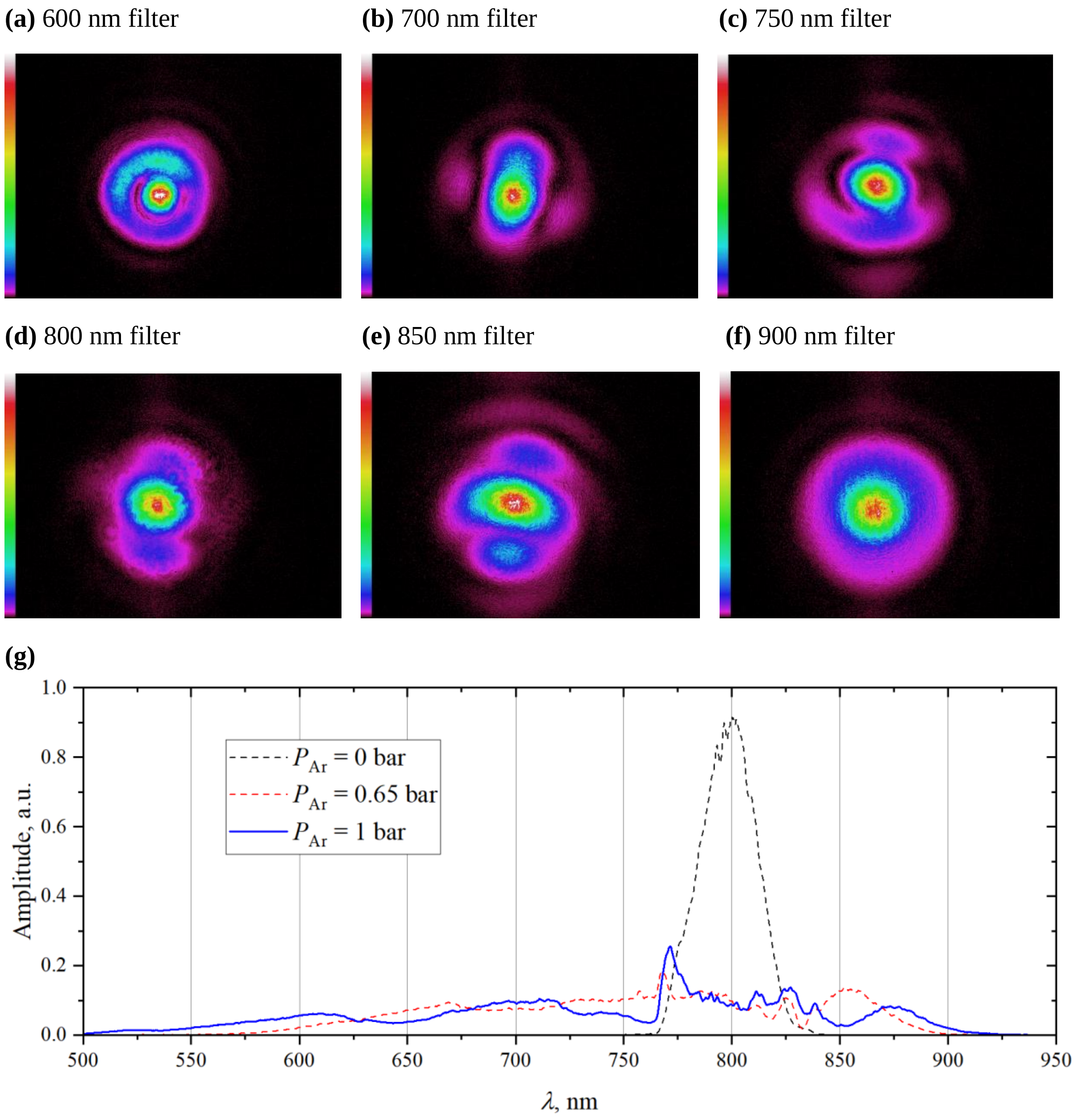

Fig. 10: Images **(a)** – **(f)** depict transverse modes with all the light filtered except for a denoted wavelength. The graph **(g)** visualizes spectra at vacuum and two different pressures. The images of the modes are related to spectrum which is visualized as a solid curve (P_{Ar} = 1 bar). The focal distance of the lens is 2 m.

Sizes of transverse modes: **(a)** x = 1.060 mm, y = 1.254 mm; **(b)** x = 1.008 mm, y = 1.531 mm; **(c)** x = 1.197 mm, y = 1.298 mm; **(d)** x = 1.258 mm, y = 1.179 mm; **(e)** x = 1.888 mm, y = 1.219 mm; **(f)** x = 1.474 mm, y = 1.478 mm.

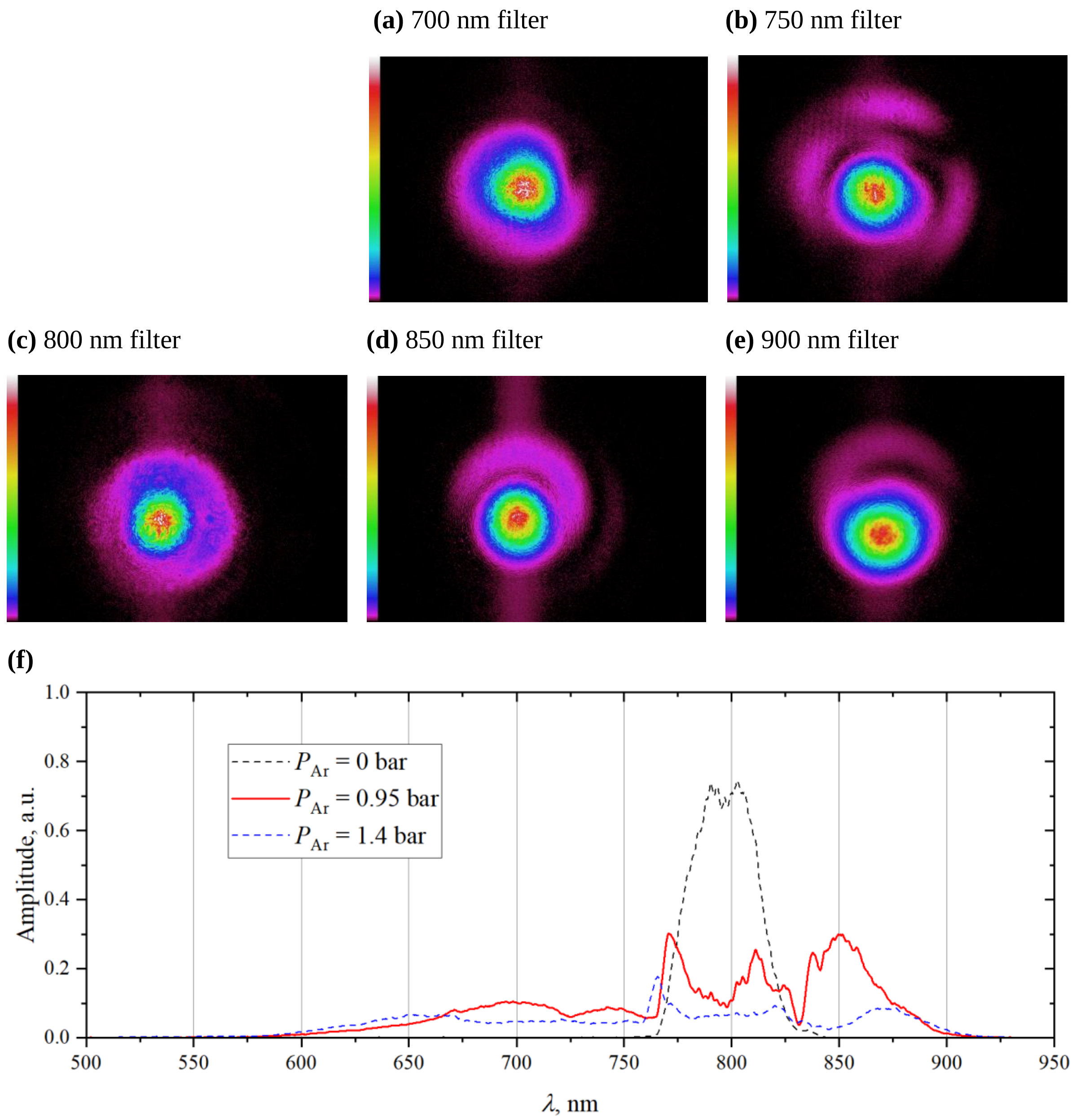

Fig. 11: Images **(a)** – **(f)** depict transverse modes with all the light filtered except for a denoted wavelength. The graph **(g)** visualizes spectra at vacuum and two different pressures. The images of the modes are related to spectrum which is visualized as a solid curve (P_{Ar} = 0.95 bar). The focal distance of the lens is 2.5 m.

Sizes of transverse modes: **(a)** x = 1.492 mm, y = 1.390 mm; **(b)** x = 1.382 mm, y = 1.329 mm;
(c) x = 1.201 mm, y = 1.342 mm; **(d)** x = 1.492 mm, y = 1.651 mm;
(e) x = 1.725 mm, y = 1.531 mm.

(a) 600 nm filter

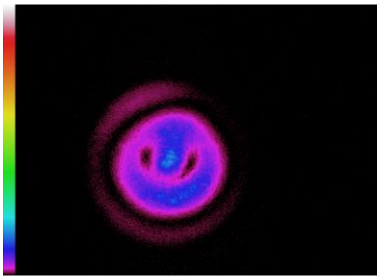

(b) 700 nm filter

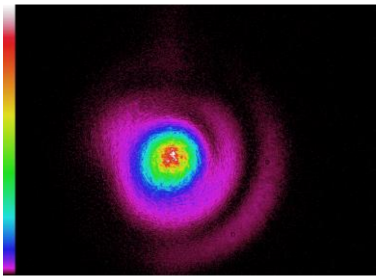

(c) 750 nm filter

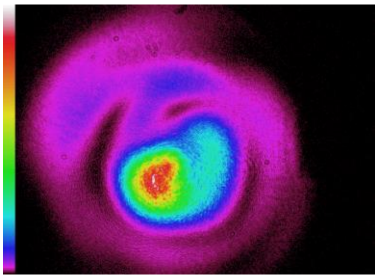

(d) 800 nm filter

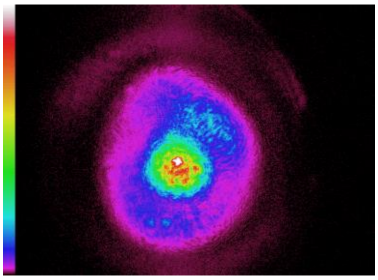

(e) 850 nm filter

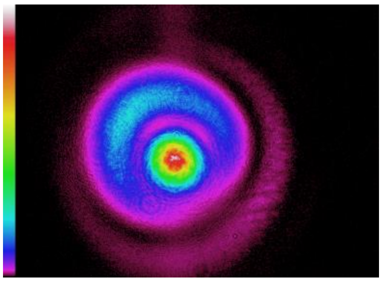

(f) 900 nm filter

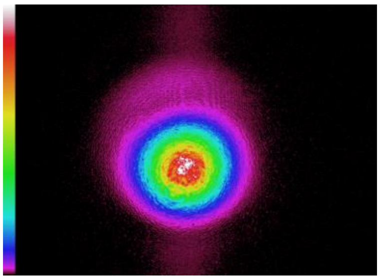

(g)

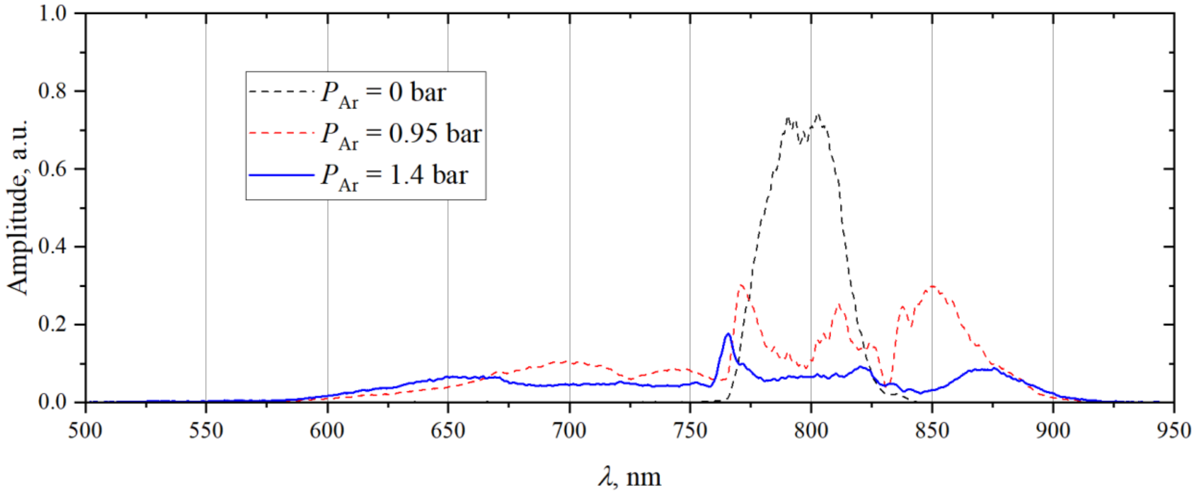

Fig. 12: Images **(a)** – **(f)** depict transverse modes with all the light filtered except for a denoted wavelength. The graph **(g)** visualizes spectra at vacuum and two different pressures. The images of the modes are related to spectrum which is visualized as a solid curve (P_{Ar} = 1.4 bar). The focal distance of the lens is 2.5 m.

Sizes of transverse modes: **(a)** x = 1.364 mm, y = 1.896 mm; **(b)** x = 1.214 mm, y = 1.214 mm; **(c)** x = 2.059 mm, y = 1.571 mm; **(d)** x = 1.241 mm, y = 1.404 mm; **(e)** x = 1.738 mm, y = 1.650 mm; **(f)** x = 1.826 mm, y = 1.681 mm.

(a) 700 nm filter

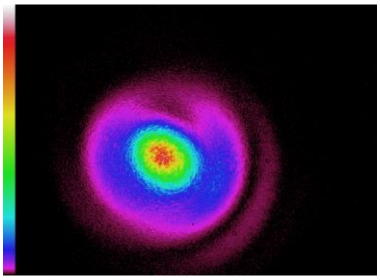

(b) 750 nm filter

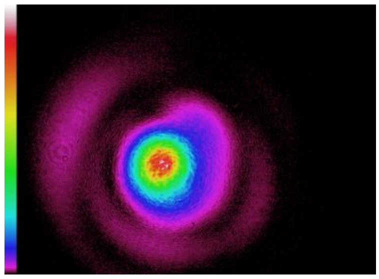

(c) 800 nm filter

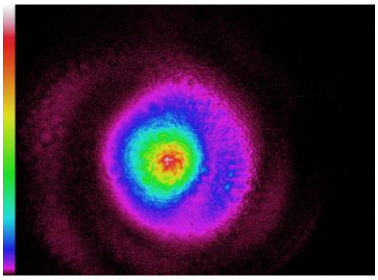

(d) 850 nm filter

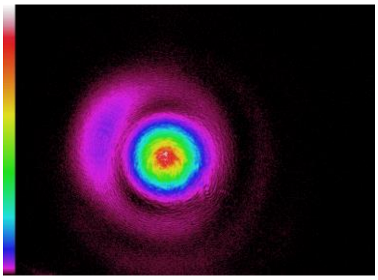

(e) 900 nm filter

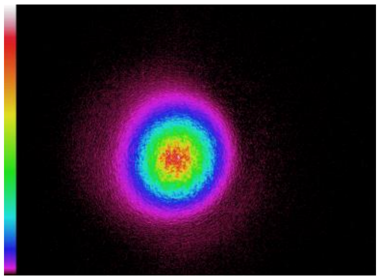

(f)

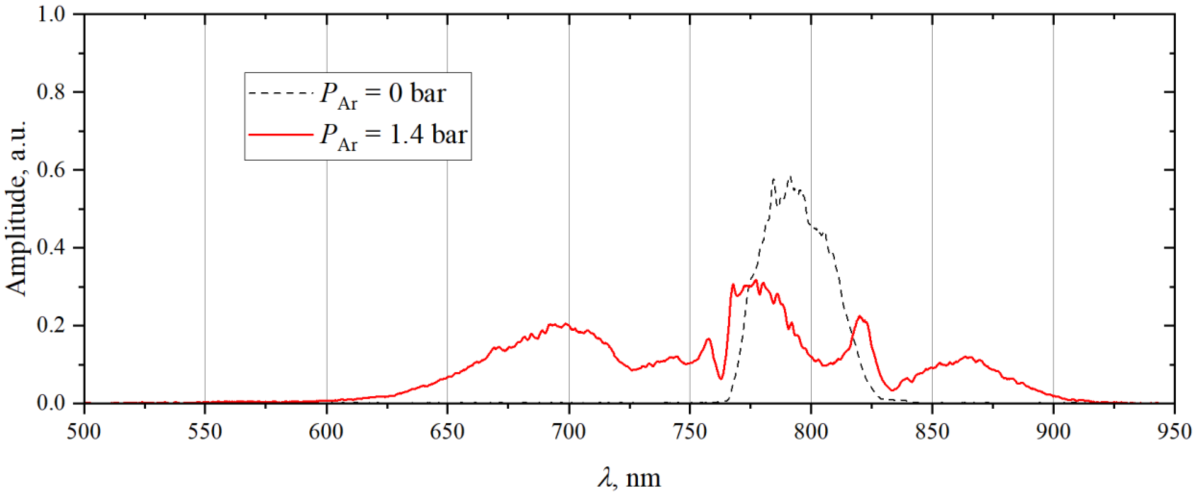

Fig. 13: Images **(a)** – **(f)** depict transverse modes with all the light filtered except for a denoted wavelength. The graph **(g)** visualizes spectra at vacuum and pressures of 1.4 bar (The pressure inside the hollow-core fiber should not exceed 1.5 bar to prevent its damage). The images of the modes are related to spectrum which is visualized as a solid curve (P_{Ar} = 1.4 bar). The focal distance of the lens is 3 m.

Sizes of transverse modes: **(a)** x = 1.492 mm, y = 1.298 mm; **(b)** x = 1.417 mm, y = 1.448 mm;
(c) x = 1.571 mm, y = 1.747 mm; **(d)** x = 1.280 mm, y = 1.241 mm;
(e) x = 1.496 mm, y = 1.685 mm.

(a) P_{Ar} = 0 bar; **(b)** P_{Ar} = 0.95 bar; **(c)** P_{Ar} = 1.4 bar;

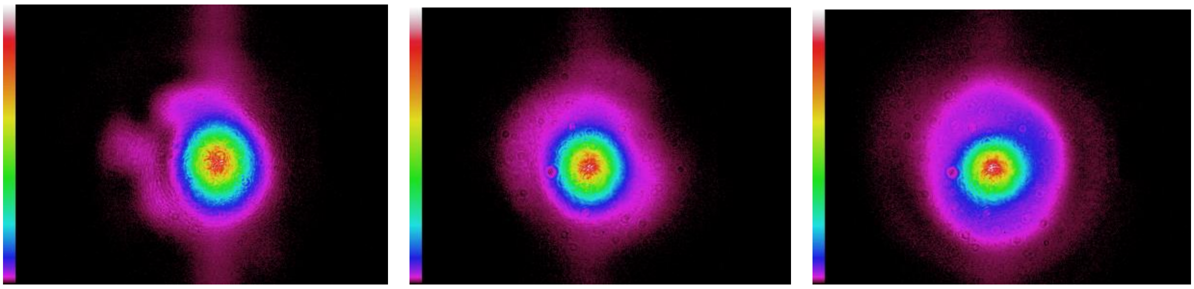

Fig. 14: Transverse mode images, F = 2.5 m lens. **(a)** x = 1.342 mm, y = 1.540 mm;
(b) x = 1.294 mm, y = 1.426 mm;
(c) x = 1.399 mm, y = 1.302 mm.

(a) P_{Ar} = 0 bar; **(b)** P_{Ar} = 1.4 bar;

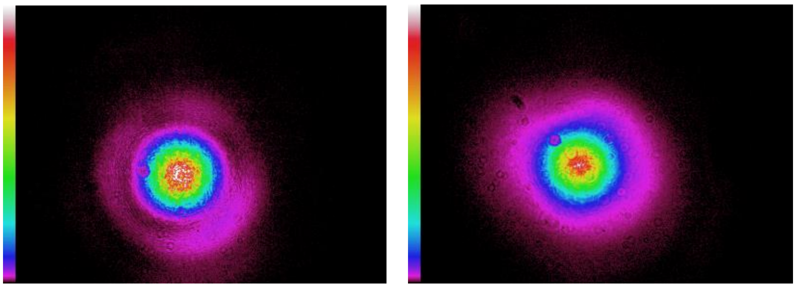

Fig. 15: Transverse mode images, F = 3 m lens.
(a) x = 1.307 mm, y = 1.338 mm;
(b) x = 1.408 mm, y = 1.421 mm.

Equipping different focal length lenses result in different losses in a fiber, the transmission coefficients are: 91% for a 2 m lens, 70% for a 2.5 m lens and 58% for a 3 m lens. Since the measurements with different lenses equipped were performed at similar pressures, we can compare the differences in spectra achieved with different lenses, the results are shown in Figure 16.

(a) 0.9 - 1 bar **(b)** 1.4 bar

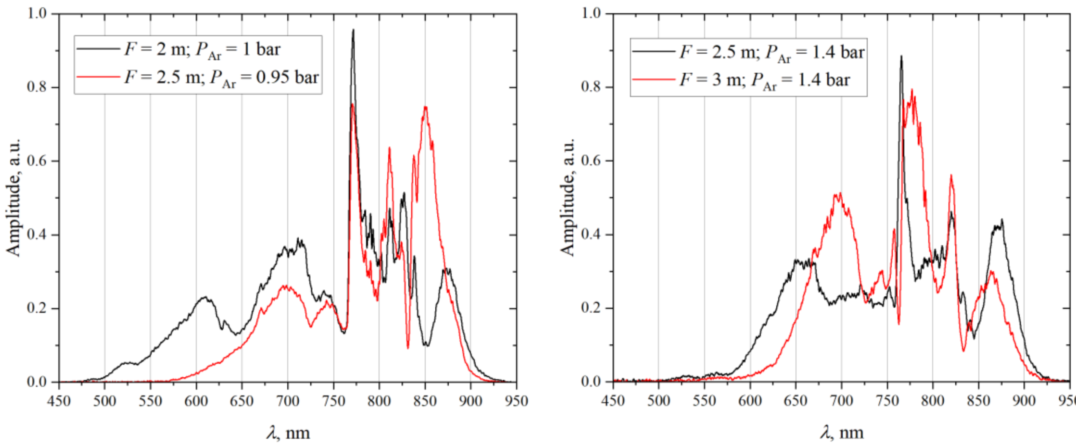

Fig. 16: Spectra measured at similar pressures, having different lenses installed.

Discussion

First, by analyzing the resulted spectra, we can state that the greater width can be achieved at a higher Ar pressure and with a shorter focal distance lens. The more noticeable spectral broadening at higher pressures may be attributed to the fact, that the nonlinear media becomes more responsive to the electric fields, more Ar molecules result in higher refractive index for higher intensities. In the case of different lenses, even though the lenses of smaller focal distances have a bigger beam divergence angle, the transverse intensity distribution is more concentrated, resulting in a stronger nonlinear response of refractive index, thus, contributing to self-phase modulation, creating a wider frequency distribution. The transmission losses for longer focal distance lenses can be attributed to the fact that the part of a wider beam profile might couple into the cladding, thus, unable to propagate inside the fiber core.

Comparing the transverse mode images, a few correlations can be noticed. Transverse mode components of smaller wavelengths (Figure 9 (a), (b); Figure 10 (b); Figure 12 (a), (c)) are far from a perfect symmetry, as well as the modes in Figure 9 (d) and Figure 10 (e). One of the possible reasons behind such results, is the interference of reflected transverse components of propagating electromagnetic waves. Since the lenses of 2 and 2.5 m focal distances result in bigger divergence angle, the reflections of the inner surface of the fiber cladding are more significant. This might explain why such asymmetry occurs at specific wavelengths. Another explanation might be the occurring polarization (since it could deform the mode to different TEM shapes [8]) because of internal reflections, again, it would depend on beam divergence and could be more drastic for specific wavelengths. One more explanation is the unperfect adjustment of the fiber. This could easily explain the deformations like in Figure 13 (b), (c) and (d), but would not explain the resulted modes seen in Figure 9 (b), Figure 10 (b) and (e) (further fiber adjustments while observing the modes mentioned above, the deformation became more noticeable while the output power was decreasing).

Conclusions

- In this work, using different focusing lenses, the transverse modes of spectrally broadened femtosecond laser radiation in gas-filled fiber were investigated. Modes appear more symmetric when a lens of a longer focal distance is used.
- With different combination of lenses and pressures inside the fiber core, different spectra were measured. Higher pressures resulted in wider spectra, as well as having a lens with shorter focal distance equipped.
- The transmission coefficients are: 91% for a 2 m lens, 70% for a 2.5 m lens and 58% for a 3 m lens.
- The best setup configuration turned out to be the one with 2.5 m focal distance lens equipped, since using this setup, most of the modes were symmetric and the acceptable 70% transmission coefficient was achieved.

References

[1] M. Nisoli, S. De Silvestri, and O. Svelto , "Generation of high energy 10 fs pulses by a new pulse compression technique", Appl. Phys. Lett. 68, 2793-2795 (1996)

[2] Weichert, Stefan (2017). Spectral broadening of 25 fs laser pulses via self-phase modulation in a neon filled hollow core fibre (DESY-THESIS--2017-017). Germany

[3] Frequency-Resolved Optical Gating: The Measurement of Ultrashort Laser Pulses. (n.d.). Google Books. https://books.google.lt/books?id=yfLIg6E69D8C

[4] Robinson, J. S., Haworth, C. A., Teng, H., Smith, R. A., Marangos, J. P., & Tisch, J. W. G. (2006). The generation of intense, transform-limited laser pulses with tunable duration from 6 to 30 fs in a differentially pumped hollow fibre. Applied Physics B, 85(4), 525-529.

[5] Miranda, O. Z. (2022). FWM in a gas-filled hollow core capillary (Doctoral dissertation, Université Bourgogne Franche-Comté).

[6] Hoffmann, Andreas & Zuerch, Michael & Spielmann, Christian. (2015). Extremely Nonlinear Optics Using Shaped Pulses Spectrally Broadened in an Argon- or Sulfur Hexafluoride-Filled Hollow-Core Fiber. Applied Sciences. 5. 1310-1322. 10.3390/app5041310.

[7] Jeong, Y. G., Piccoli, R., Ferachou, D., Cardin, V., Chini, M., Hädrich, S., ... & Razzari, L. (2018). Direct compression of 170-fs 50-cycle pulses down to 1.5 cycles with 70% transmission. Scientific reports, 8(1), 1-6.

[8] Zhang, H., Mao, B., Han, Y., Yang, K., Wang, Z., & Liu, Y. (2019). Generation of orbital angular momentum mode using a single cylindrical vector mode based on mode selective coupler. Optical Fiber Technology, 52, 101934.